

Controlling the degree of hydrophilicity / hydrophobicity of semiconductor surfaces via porosification and metal deposition

E.V. Monaico¹, S. Busuioc¹, I.M. Tiginyanu^{1,2}

¹ Technical University of Moldova, National Center for Materials Study and Testing, Stefan cel Mare av. 168, MD-2004, Chisinau, Republic of Moldova

² Academy of Sciences of Moldova, Stefan cel Mare av. 1, MD-2001, Chisinau, Republic of Moldova

Abstract— In this paper we present a systematic study of bulk GaAs wafers and gold-decorated GaAs surfaces exhibiting hydrophilic and hydrophobic behaviors. The wetting properties can be switched to superhydrophilicity and superhydrophobicity by simple electrochemical etching providing engineered porous morphologies. The results open interesting technological perspectives for the exploitation of GaAs surfaces.

Keywords— wetting, porous, electrodeposition, contact angle, hydrophilic-hydrophobic.

I. INTRODUCTION

The investigation of wetting properties (hydrophobicity and hydrophilicity) via measurements of contact angle (CA), give the information about the ability of liquids to flow on the surface or to form droplets. It is considered that a large value of contact angle (above 90 degrees) reflects a hydrophobic surface, while a low value of contact angle reflects a hydrophilic surface. As a rule, surfaces showing contact angle lower than 10 or higher than 150 are classified to superhydrophilic or superhydrophobic respectively. Numerous studies demonstrated that contact angle can be influenced by the micro- and nanoscale morphology of the surface, and by an engineered design of the surface roughness.

Among III-V semiconductor compounds, gallium arsenide (GaAs) represent a class of important materials for high frequency microelectronic and optoelectronics industries such as: telecommunication lasers [1,2], imaging [3,4], photodetectors [6], sensors [6] and solar cells [7,8]. Nowadays, hydro insulation is very important technological step intended to protect electrical components embedded in consumer devices, such as computers, smartphones, smart watches, medical examination devices and more. To protect the microchips from contact with water, hydrophobic polymers such as polydimethylsiloxane (PDMS) are usually used, but they are characterized by low thermal conductivity [9,10] leading to poor heat dissipation [11]. The idea of III-V semiconductor impermeability has been previously re-

ported, involving the transfer of epitaxially grown III-V structures to flexible and impermeable substrates such as PDMS [12]. However, these processes are complicated from the point of view of realization. An alternative approach could serve surface nanostructuring, which has been shown to be an effective way to control the hydrophobicity [13] and suppress ice formation [14].

Over the last two decades, it was demonstrated that electrochemistry represents not only a cost-effective approach for nanostructuring of semiconductor crystals at high etch rate, but also an environmentally friendly tool due to controlled electrochemical etching in salty water [15-18]. It is important to point out that GaAs is a material that has been shown to differ from other semiconductor compounds by the diversification of obtained morphologies. It should be noted that the intersection of pores was observed, for the first time in GaAs [19]. In addition, an absolutely new morphology namely, tetrahedron-like interconnected voids in GaAs were reported [20]. Moreover, GaAs with crystallographic orientation (111) exhibits polarity with two polar surfaces: (111)A (Ga-atoms side) and (111)B (As-atoms side). Recently, a comparative study of the electrochemical etching in neutral NaCl and acidic HNO₃ based aqueous electrolytes of (111)A and (111)B GaAs surfaces was performed, demonstrating the formation of tilted or perpendicular to the surface pores and even nanowires [21,22].

It is worth to mention that functionalization of surfaces with metallic dots has attracted great research interest in the fields of medicine, chemistry and biology due to surface enhanced Raman scattering [23-25]. Deposition of nanodots can significantly modify the surface roughness leading to appearance of new properties. In case the deposition is performed on semiconductor substrates or porous matrices that possess good electrical conductivity, electroplating of metal dots proves to be the most efficient methods.

The goal of this paper is a systematic study of bulk GaAs wafers with two different crystallographic orientations and gold decorated GaAs surfaces, which shows hydrophilic or hydrophobic behaviors. The wetting properties can be switched by simple electrochemical etching leading to engineered porous morphologies.

II. EXPERIMENTAL DETAILS

Crystalline 500- μm thick Si-doped n-GaAs (001) and two side polished (111) wafers with the free electron concentration of $3 \times 10^{18} \text{ cm}^{-3}$ and $2 \times 10^{18} \text{ cm}^{-3}$ respectively, supplied by MaTeck GmbH, Germany were used as substrates. As a first step, the samples were sonicated in acetone for 5 min, cleaned in distilled water and dried. With the aim to remove the native oxide from the surface, the samples were dipped in a HCl/H₂O solution with the ratio (1:3) for 2 min.

Electrochemical deposition of gold was performed in a commercially available gold bath containing 5g/l Au (DODUCO, Germany). The electroplating of Au was carried out at $T = 25 \text{ }^\circ\text{C}$ in a common two-electrode plating cell where the semiconductor sample served as working electrode, while a platinum wire was used as counter electrode. A pulsed rectangular shape negative voltage of -15 V was provided by a home-made generator. The metal species were electrochemically reduced on the sample surface being in contact with the electrolyte, during the pulse time of 50 μs and 300 μs . A delay time as long as one second was kept after each pulse. The total time of the electroplating was 300 sec.

Gold films were also deposited by sputtering for comparison purposes using a Cressington Sputter Coater 108 Auto instrument under current intensity of 40 mA for 15, 30, and 45 sec at the distance of 45 mm between the sample and gold target, resulting in 7, 13, and 50 nm thickness of the deposited film respectively.

Electrochemical etching was carried out in potentiostatic regime at room temperature ($T=25 \text{ }^\circ\text{C}$) at applied anodization voltage 3.5 V during 15 min, resulting in the formation of porous layer with the thickness around 50 μm . The electrical contacts to the sample were performed with silver paste, and then the sample was pressed against an O-ring in a Teflon cell with the 0.2 cm^2 area exposed to the 1M HNO₃ electrolyte. The experiments were performed in two-electrode configuration: a Pt mesh with the surface area of 6 cm^2 acting as counter electrode while the sample acted as working electrode.

The morphology of samples was investigated by using scanning electron microscope (SEM) TESCAN Vega TS 5130 MM equipped with an Oxford Instruments INCA Energy EDX system operated at 20 kV for chemical composition analysis.

Contact angle measurements were carried out with water using the KRUSS DSA25 (drop shape analyzer) equipped with a camera. The sample was illuminated from behind so that the shadow contour of the substrate-drop contact was visible and well highlighted to allow the software to determine the contact angle.

III. RESULTS AND DISCUSSIONS

To establish how the deposition of metal influence the wetting properties of semiconductor crystals surface (GaAs in our case) we have investigated the contact angle of bulk GaAs substrates and bulk GaAs decorated with deposited gold nanodots.

The measured contact angle of bulk n-GaAs substrate is 80.4° as is shown in Fig. 1b. As can see from SEM image in Fig. 1c, the electrochemical deposition of gold on bulk n-GaAs substrate with pulse duration of 50 μs resulted in formation of thin layer consisting of closely packed Au nanodots. Thorough analysis of the SEM image presented in Fig. 1c shows that the transverse dimensions of the dots do not exceed 20 nm. The similar results were earlier reported for Au deposition on porous n-InP and n-GaP semiconductors compounds [26]. In this case, the measured contact angle decreased to 73.9° (see Fig. 1d) due to the small voids between the deposited Au dots.

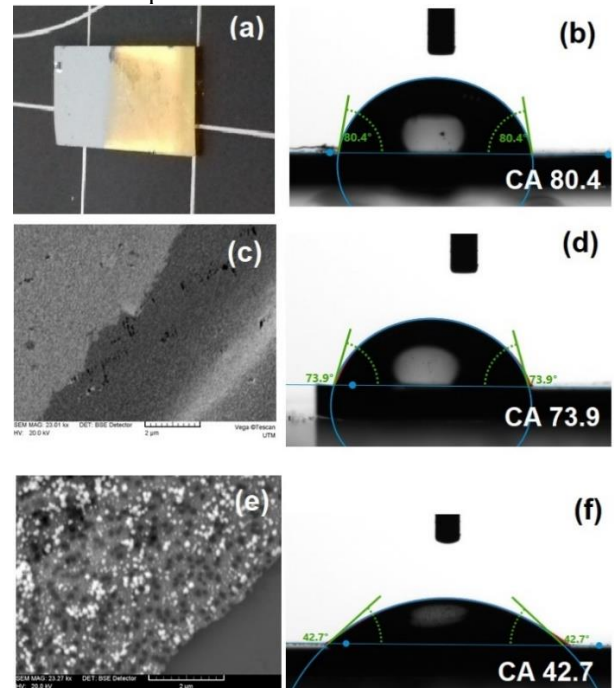


Fig. 1 Photo of electrochemically deposited Au film at pulse duration 300 μs (right side) on bulk GaAs (left side). SEM images of deposited gold film at pulse duration 50 μs (c) and 300 μs (e). Measured contact angle for bulk GaAs surface (b), deposited film with pulse duration 50 μs (d) and 300 μs (f)

The increase of the pulse duration up to 300 μs during electrochemical deposition leads to the formation of perforated Au membrane on the surface of GaAs semiconductor substrate with the thickness about 100 nm (Fig. 1e). The resulted contact angle about 42.7° was registered indicating

hydrophilic properties of GaAs surface decorated by perforated gold membrane. The increase in hydrophilicity is mainly attributed to the difference in both the chemical properties of GaAs surface and its surface morphology.

The formation of pores in deposited Au film can be explained in the following way: applied voltage pulses with longer duration led to visible bubble formation at the GaAs surface during electroplating. It is considered that hydrogen or oxygen liberations are the major cause of these bubble formation. Formed bubbles on the surface of the sample reduce their effective surface area, resulting in fluctuations of current density and affecting the deposition process in these places. As a result, the gold is not deposited on places occupied by these bubbles on the GaAs surface.

To compare the impact of Au distribution during the deposition, an alternative method was involved. Three samples with Au film thickness of 7 nm, 13 nm, and 25 nm were prepared using sputtering. No change in the morphology was evidenced after deposition of Au via SEM investigation. In spite of this, the decrease of contact angle from 80.4° for bulk GaAs to 70.9° for GaAs/Au with thicknesses of 7 nm was observed as is illustrated in Fig. 2b. It can be explained by the fact that deposition for such small thickness occurs not uniformly on the entire surface but via islands. Further increase of the deposition thickness leads to the growth of islands till their interconnection and formation of continuous gold layer occurs. As a result, the value of the contact angle is increased up to 71.3° and 72.8° for 13 nm and 25 nm respectively (see Fig. 2c,d).

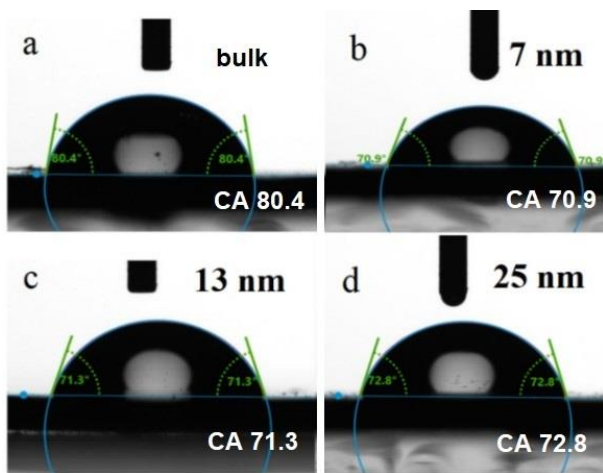


Fig. 2 Measured contact angle for bulk n-GaAs (a) and sputtered gold film with thickness of 7 nm (b), 13 nm (c), and 25 nm in (d) on GaAs surface

Higher uniformity of the Au film deposited via sputtering is explained taking into account the polarization curves

measured at the beginning of anodization of bulk GaAs and bulk GaAs with deposited gold, reported in our recent work [27]. It was shown that anodization of bulk GaAs under 4 V leads to higher current density resulting in the formation of porous layer. However, in the case of bulk GaAs samples with electrochemically deposited Au nanoparticulate film with different durations of deposition leads to a significant decrease in the current intensity, especially for deposition at $50 \mu\text{s}$ width of the pulse [27]. It can be explained by formation of very small voids between the deposited nanodots, and thus a small amount of the electrolyte during electrochemical etching enters in contact with the surface of the bulk GaAs. This statement is confirmed by the investigation of deposited gold film via sputtering resulting in the formation of more continuous film leading to practically no reaction at the semiconductor-electrolyte interface [27].

Introducing porosity on the semiconductor surface is another way to control the wetting properties. We investigated porous layer obtained via anodization of both (111)GaAs surfaces. It was recently showed that anodization on different (111)GaAs surfaces resulting in different orientation of pores to the surface [21,22]. On the (111)A GaAs surface the pores interconnect each other and are tilted (see Fig. 3a). Measured contact angle showed that the value of contact angle increased to 137.5° (see Fig. 3d), close to those of super-hydrophobic, comparatively to the bulk surface (95.4°). The situation is contrary in the case of nanostructured (111)B GaAs surface exhibiting pores and nanowires perpendicular to the surface (see Fig. 3b). This morphology gives a contact angle of 37.5° indicating strong hydrophilic properties (Fig. 3e).

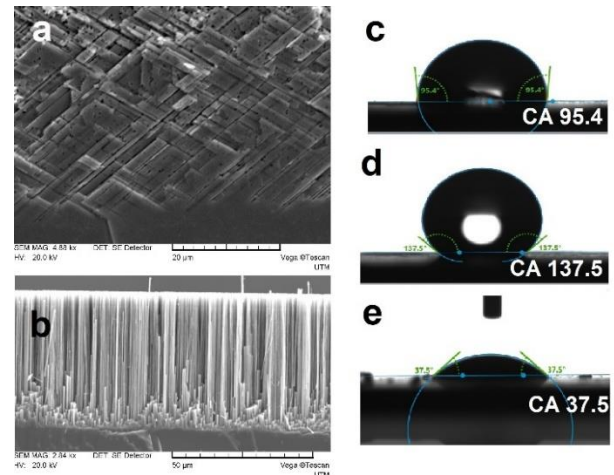


Fig. 3 SEM images of anodized n-GaAs (111)A and (111)B surfaces at applied potential 3.5 V in 1M HNO_3 in (a) and (b) respectively. Measured contact angle for bulk (c), porous (111)A surface in (d) and porous (111)B surface in (e)

IV. CONCLUSIONS

In this work we showed that the wetting properties of GaAs surface can be engineered by electrochemical deposition of gold nanodots. The increase in hydrophilicity was demonstrated for deposited gold with longer pulse duration leading to the formation of perforated Au membrane on the GaAs surface. The introduced porosity on the semiconductor surface gives the possibility to control the wetting properties of the GaAs surface. The morphology of pores, tilted or perpendicular to the surface, play an important role in switching from the hydrophobic to hydrophilic properties.

ACKNOWLEDGMENT

This work received partial funding from the European Commission under the H2020 grant #810652 ‘NanoMedTwin’ and PostDoc Grant #21.00208.5007.15/PD.

CONFLICT OF INTEREST

The authors declare that they have no conflict of interest.

REFERENCES

1. Ustinov VM, Zhukov AE (2000) GaAs-based long-wavelength lasers. *Semicond. Sci. Technol.* 15:R41–R54 DOI 10.1049/ip-cds:20030959
2. Liu HY et al. (2011) Long-wavelength InAs/GaAs quantum-dot laser diode monolithically grown on Ge substrate. *Nat. Photon.* 5:416–419 DOI 10.1038/nphoton.2011.120
3. Ng WH et al. (2007) Broadband quantum cascade laser emitting from 7.2 to 8.4 μm operating up to 340 K. *J. Appl. Phys.* 101:046103 DOI 10.1063/1.2472196
4. Colley CS et al. (2007) Mid-infrared optical coherence tomography. *Rev. Sci. Instrum.* 78:123108 DOI 10.1038/s41377-019-0122-5
5. Krishna S (2005) Quantum dots-in-a-well infrared photodetectors. *J. Phys. D: Appl. Phys.* 38:2142–2150
6. Potyrailo RA et al. (2015) Towards outperforming conventional sensor arrays with fabricated individual photonic vapour sensors inspired by Morpho butterflies. *Nat. Commun.* 6:7959
7. Holm JV et al. (2003) Surface-passivated GaAsP single-nanowire solar cells exceeding 10% efficiency grown on silicon. *Nat. Commun.* 4:1498 DOI 10.1038/ncomms2510
8. Fan Z et al. (2009) Three-dimensional nanopillar-array photovoltaics on low-cost and flexible substrates. *Nat. Mater.* 8:648–653 DOI 10.1038/nmat2493
9. Tang GY, Yang C, Chai CK, Gong HQ (2004) Numerical analysis of the thermal effect on electroosmotic flow and electrokinetic mass transport in microchannels. *Anal. Chim. Acta.* 507:27–37
10. Erickson D, Sinton, D, Li D (2003) Joule heating and heat transfer in poly(dimethylsiloxane) microfluidic systems. *Lab Chip* 3:141–149 DOI 10.1039/B306158B
11. Zhang Y, Bao N, Yu XD et al. (2004) Improvement of heat dissipation for polydimethylsiloxane microchip electrophoresis. *J. Chromatogr. A* 1057:247–251 DOI 10.1016/j.chroma.2004.09.009
12. Kim R-H et al. (2010) Waterproof AlInGaP optoelectronics on stretchable substrates with applications in biomedicine and robotics. *Nat. Mater.* 9:929–937 DOI 10.1038/nmat2879
13. Lu Y et al. (2015) Robust self-cleaning surfaces that function when exposed to either air or oil. *Science* 347:1132–1135
14. Kim P et al. (2012) Liquid-infused nanostructured surfaces with extreme anti-ice and anti-frost performance. *ACS Nano* 6, 6569–6577 DOI 10.1021/nn302310q
15. Monaco E, Tiginyanu I, Ursaki V (2020) Porous semiconductor compounds. *Semiconductor Science and Technology*, 35:103001 DOI 10.1088/1361-6641/ab9477
16. Tiginyanu IM, Ursaki VV, Monaco E et al. (2007) Pore Etching in III-V and II-VI Semiconductor Compounds in Neutral Electrolyte. *Electrochem. Solid-State Lett.*, 10(11):D127-D129.
17. Tiginyanu IM, Monaco E, Albu S, Ursaki VV (2007) Environmentally friendly approach for nonlithographic nanostructuring of materials. *Phys. Stat. Sol. (RRL)*, 1(3):98–100
18. Volciuc O, Monaco E, Enachi M, Ursaki VV et al. (2011) Morphology, luminescence, and electrical resistance response to H₂ and CO gas exposure of porous InP membranes prepared by electrochemistry in a neutral electrolyte. *Applied Surface Science.* 257(3):827-831 DOI 10.1016/j.apsusc.2010.07.074
19. Langa S, Carstensen J, Christophersen M et al. (2001) Observation of crossing pores in anodically etched n-GaAs *Applied Physics Letters* 78(8):1074-1076 DOI 10.1063/1.1350433
20. Langa S, Carstensen J, Tiginyanu IM et al. (2002) Formation of Tetrahedron-Like Pores during Anodic Etching of (100) Oriented n-GaAs *Electrochemical and Solid-State Letters*, 5(1):C14-C17 DOI 10.1149/1.1423803
21. Monaco EI, Monaco EV, Ursaki VV et al. (2020) Electrochemical nanostructuring of (111) oriented GaAs crystals: from porous structures to nanowires. *Beilstein J. Nanotechnol.* 11:966–975. DOI 10.3762/BJNANO.11.81
22. Monaco EI, Monaco EV, Ursaki VV, Tiginyanu IM (2021) Evolution of pore growth in GaAs in transitory anodization regime from one applied voltage to another one. *Journal of Surface Engineering and Applied Electrochemistry.* 57(2):65–172
23. Yuanyuan X, Yunwen W, Liwen et al. (2020) Two-step Electrodeposited 3D Ni Nancone Supported Au. *Journal of The Electrochemical Society* 167:142502 DOI 10.1149/1945-7111/abc0aa
24. Jiacheng Zhu, Li Sun, Yuejin Shan, Yuan Zhi, et al. (2021) Green preparation of silver nanofilms as SERS-active substrates for Rhodamine 6G detection. *Vacuum* 187:110096 DOI 10.1016/j.vacuum.2021.110096
25. Arfat P, Ni Luh WS et al. (2021) Review—Nanopillar Structure in the Direction of Optical Biosensor On-Chip Integration *J. Electrochem. Soc.* 168:057505 DOI 10.1149/1945-7111/abfb3a
26. Tiginyanu I, Monaco E, Nielsch K (2015) Self-assembled monolayers of Au nanodots deposited on porous semiconductor structures. *ECS Electrochemistry Letters*, 4:D8-D10 DOI 10.1149/2.0041504eel
27. Monaco EV, Monaco EI, Ursaki VV, Tiginyanu IM (2020) Free-Standing Large-Area Nanoperforated Gold Membranes Fabricated by Hopping Electrodeposition. *ECS Journal of Solid State Science and Technology.* 9: 064010 DOI 10.1149/2162-8777/aba6a2

Author: dr. Eduard Monaco
 Institute: Technical University of Moldova
 Street: Stefan cel Mare Avenue 168
 City: Chisinau, MD-2004
 Country: Republic of Moldova
 Email: eduard.monaco@cstm.utm.md

